

Natural multimerization rules the performance of affinity-based physical hydrogels for stem cell encapsulation and differentiation

Cláudia S.M. Fernandes¹, André L. Rodrigues², Vitor D. Alves³, Tiago G. Fernandes², Ana Sofia Pina^{1}, Ana Cecília A. Roque^{1*}*

¹ UCIBIO, Departamento de Química, Faculdade de Ciências e Tecnologia, Universidade NOVA de Lisboa, Campus Caparica, 2829-516 Caparica, Portugal
E-mail: ana.pina@fct.unl.pt and cecilia.roque@fct.unl.pt

² Department of Bioengineering, iBB – Institute for Bioengineering and Biosciences, Instituto Superior Técnico, Universidade de Lisboa, Av. Rovisco Pais, 049-001 Lisboa, Portugal

³ LEAF, Linking Landscape, Environment, Agriculture and Food, Instituto Superior de Agronomia, Universidade de Lisboa, Tapada da Ajuda, 1349-017 Lisboa, Portugal.

Keywords: physical hydrogels, stem cell encapsulation, stem cell differentiation, multicomponent self-assembly, avidin and biotin

Abstract

Tissue engineering and stem cell research greatly benefit from cell encapsulation within hydrogels, as it promotes cell expansion and differentiation.

Affinity-triggered hydrogels, an appealing solution for mild cell encapsulation, rely on selective interactions between ligand and target, and also on the multivalent presentation of these two components. Although these hydrogels represent a versatile option to generate dynamic, tunable and highly functional materials, the design of hydrogel properties based on affinity and multivalency remains challenging and unstudied. Here, the avidin-biotin affinity pair, with the highest reported affinity constant, is used to address this challenge. It is demonstrated that the binding between the affinity hydrogel components is influenced by the multivalent display selected. In addition, the natural multivalency of the interaction must be obeyed to yield robust multicomponent synthetic protein hydrogels. Hydrogel's

resistance to erosion depends on the right stoichiometric match between the hydrogel components. The developed affinity-triggered hydrogels are biocompatible, and support encapsulation of induced pluripotent stem cells and their successful differentiation into a neural cell line. This principle can be generalized to other affinity pairs using multimeric proteins, yielding biomaterials with controlled performance.

1. Introduction

Interfacing chemistry and biology has generated incredible biomedical tools, in particular in the field of biomaterials for cell encapsulation and differentiation¹⁻³. Pluripotent stem cells are ideal for personalized cell therapies since they can potentially differentiate into any cell type of the human body⁴⁻⁶. Stem cells demonstrate good clinical results in alleviating, for example, the motor symptoms of neurological disorders as Parkinson's disease⁴. However, cell replacement therapies are still limited by the large number of high-quality cells needed, as *in vivo* survival of transplanted cells and functional integration are typically very low⁶. As an example, only 1–5% of midbrain dopaminergic neurons used for cell replacement therapy treatment survive after striatal transplantation⁷. To address this issue, cell encapsulation has been used to promote cell expansion and differentiation.

Cell encapsulation is typically achieved with biomaterials mimicking the *in vivo* conditions conferred by the extracellular matrix (ECM). The ECM is composed by different multifunctional proteins that provide cells with biochemical and structural cues for their growth, multiplication and differentiation⁸. Several natural materials have been used to provide cells with such cues. In particular, Matrigel[®] is a commercially available cell culture substrate⁹ used as a matrix for *in vitro* cell and tissue culture despite its non-

reproducible and poorly defined composition¹⁰⁻¹². In addition, it can also lose its biological activity during processing¹³ and be immunogenic^{8,14}. These disadvantages have led many scientists to develop innovative strategies to mimic the ECM, which have been extensively reviewed elsewhere^{8,15-17}.

Affinity-triggered hydrogels are a class of protein-based hydrogels that closely resemble the dynamic behaviour of the ECM¹⁸, as they can be tailored towards biocompatibility, hydrophilicity and biodegradability, while also tuning the porosity, mechanical properties and rate of degradation^{14,19,20}. The wide range of available binding constants from known affinity pairs, the selective molecular recognition of affinity interactions, and the existence of diverse multivalent systems to display the ligand and the receptor – from fully biological to synthetic - make affinity-triggered hydrogels a versatile tool to generate controllable, dynamic, tunable and highly functional materials²¹. Various ligand/receptor affinity pairs have been explored to assemble hydrogels for tissue engineering applications, namely TIP1/TIP1-binding peptides^{22,23}, WW/proline-rich peptides²⁴⁻²⁸, and gyrase/coumermycin²⁹, as well as host/guest supramolecular pairs^{30,31}. Multivalency is achieved through (i) the presentation of the ligand or receptor as tandem displays (e.g. recombinant expression of ligand displayed in tandem with suitable linkers), (ii) the chemical conjugation of the ligand and/or receptor to multimeric polymers (e.g. branched polyethyleneglycol (PEG)), or (iii) the use of naturally occurring multimeric ligands or receptors. The reported examples of affinity-triggered hydrogels are based on trial and error approaches. Firstly, it is assumed that higher component multivalency promotes crosslinking and hydrogel's robustness³². Secondly, only the observed binding constant of ligand-receptor in solution is considered, and not the binding interactions established in the real hydrogel system where multivalent polymers and linkers exist, giving rise to stereo-hindrance and or avidity effects. The

importance of establishing design rules to yield multicomponent protein hydrogels with predictable properties has been acknowledged in systems using tandem display of engineered protein components^{25,33}. However, considering the palette of multimeric proteins that Nature has to offer, it is inspirational to take further these examples towards biomaterials engineering.

The natural avidin-biotin affinity pair has the highest reported affinity constant (up to 10^{15} M⁻¹)^{34,35} and is a valuable tool in innumerable applications³⁶. Avidin (67 kDa) is a naturally occurring tetrameric protein, whereas biotin is a small molecule (244 Da) that can be chemically conjugated to different matrices. The interaction between avidin and biotin is unaffected by temperature, pH, organic solvents and denaturing agents, which makes this affinity pair an extremely interesting platform to generate stable chemical-biology interfaces. The affinity pair avidin-biotin promotes crosslinking in multicomponent hydrogels, where biotin-multivalency was given by linear PEG^{34,37} or hyaluronic acid³⁸. In these pioneering examples, the strong interaction between avidin and biotin was successfully explored to generate hydrogels, but the affinity and avidity present in the multicomponent system was disregarded during materials design.

Here, it is shown that the natural multivalency of the interaction between avidin and biotin can be mimicked in hydrogel assembly. This is achieved by tuning the multivalent presentation of the synthetic component (biotin-derivatized PEG) yielding materials with controlled performance. Such materials, which self-assemble instantaneously, encapsulate pluripotent stem cells and support neural commitment in defined xeno-free conditions, by ensuring cell expansion and differentiation. This work provides the design rules for affinity-based hydrogels, while also opening opportunities in the field of neural cell replacement therapy.

2. Materials and Methods

2.1 Materials

Linear PEG functionalized with NHS moiety (1120000-2) was purchased from Rapp Polymere. The molecules 4-arm PEG functionalized with NHS moiety (SUNBRIGHT® PTE-200HS) and 8-arm PEG functionalized with NHS moiety (SUNBRIGHT® HGEO-200GS) were purchased from NOF Europe. Pierce™ Avidin (21128) was purchased from ThermoFischer Scientific. Biotin cadaverine (RL-2030) was acquired from Iris Biotech and Spectra/Por 7 Dialysis Tubing 10 kDa MWCO (132120) from Spectrum. The iPSC medium used was TeSR™2 Basal medium (#05861) from StemCell Technologies, DMEM medium (high glucose) (12800-082), fetal bovine serum (FBS) (10270-106), (3-(4,5-Dimethylthiazol-2-yl)-2,5-Diphenyltetrazolium Bromide) (MTT) (M6494) were purchased from Life Technologies. Fibroblast cells (NCTC clone 929 [L cell, L-929, derivative of Strain L] ATCC® CCL-1™) were purchased from ATCC.

2.2 Methods

2.2.1 Synthesis and characterization of biotinylated PEG oligomers

Biotin cadaverin, an amine-terminated biotin, was used to functionalize linear, 4-arm and 8-arm PEG molecules with terminal NHS groups. The PEG molecules were dissolved in PBS (20 mM sodium phosphate, 150 mM NaCl, pH 7.4). PEG solutions were then mixed with a 10-molar excess of biotin regarding the NHS groups of the PEG molecules. For example, 0.1 g of PEG-[NHS]₄ was dissolved in 1 ml of PBS and 0.066 g of biotin cadaverin was dissolved in 1 ml PBS. Both solutions were mixed and incubated for 16 hours at 4 °C with rotational agitation (40 rpm), and then dialyzed against water using a dialysis membrane

with a molecular weight cut-off of 10 kDa at room temperature. After dialysis, the biotin-modified PEG molecules were frozen at -80 °C and lyophilized.

The biotin-modified PEG molecules were characterized by FTIR-ATR and induced couple plasma (ICP). FTIR-ATR spectra (16 scans) were recorded in the range 400-4000 cm^{-1} on a PerkinElmer FT-IR Spectrometer Spectrum Two, using the UATR Two module. Samples were analysed using a L160-1742 tip, with a force gauge of 80-85. Biotin has one sulfur element in its structure and ICP was used to quantify the amount of sulfur in the samples. Samples (1 mg/ml in water) were analysed on a Horiba Jobin Yvon ULTIMA sequential ICP and Horiba Jobin Yvon ICP Analyst 5.4 software, using monochromator with a Czerny Turner spectrometer and Argon. The estimated degree of functionalization of the linear, 4-arm and 8-arm biotin-functionalized PEG molecules, was $(97 \pm 3)\%$ for PEG-[biotin]₂, $(109 \pm 9)\%$ for PEG-[biotin]₄ and $(95 \pm 2)\%$ for PEG-[biotin]₈.

2.2.2 Affinity constant determination

Avidin was conjugated with fluorescein isothiocyanate (FITC) to allow the determination of the affinity constant by microscale thermophoresis (MST). FITC was dissolved in a small volume of DMF, to a total of 25-excess molar to the amount of avidin. The previous solution was added to the avidin solution (2 mg/ml in 0.1 M sodium carbonate-bicarbonate pH 9.1). The reaction occurred for 24 hours at 4 °C, with agitation (40 rpm). To separate non-reacted fluorescein from fluorescently probed protein, the mixture was dialyzed against PBS using a dialysis membrane with a molecular weight cut-off of 10 kDa. The protein concentration and the efficiency of FITC-labelling were determined according to the supplier's instructions. The final protein concentration was calculated as 18.5 μM with a modification of 1.4 mol fluorescein/mol avidin.

The affinity constants between PEG-biotin molecules and fluorescently labelled avidin were determined by MST. The FITC-avidin solution was diluted to 60 nM with PBS. The biotinylated PEG molecules were dissolved in PBS, and a series of sixteen 1:2 serial dilutions were prepared in the same buffer, with a range of concentrations between 2.5 and 7.8×10^{-5} mM, to a total volume of 20 μ l. Each ligand dilution was mixed with 20 μ l of FITC-avidin solution and loaded in appropriate capillaries in independent triplicate (Monolith NT.115 Standard Capillaries). The equipment used was a Monolith NT.115 instrument (NanoTemper Technologies), working at an ambient temperature of 25°C, with parameters adjusted to 20 % LED power and 20 % MST power. The affinity constant is calculated by the software, by fitting the experimental data to the Hill model, with a response evaluation at 10s.

2.2.3 Hydrogel formation and characterization

Biotinylated PEG oligomers and avidin were both dissolved separately in PBS. Equal volumes of both components were mixed in order to have a final concentration of each component of 0.1%, 0.5%, 1%, 2.5%, 5% and 10% (w/v). The gelation of the mixed components was observed immediately.

To assess the erosion profile of the assembled gels, 50 μ l hydrogels were formed. The weight of the hydrogel was recorded at the beginning of the study. PBS was added to the vial containing the hydrogel and completely removed after 10 minutes. The new weight was measured, and fresh PBS was added to the vial. This was repeated until a maximum of three months every five days, in duplicate.

To assess the binding competition between free biotin and PEG conjugated biotin in hydrogels, hydrogel (50 μ l) was formed, and after 16 hours, it was immersed in a solution

containing 2 mg biotin/ml in PBS. The erosion profile was assessed by weight measurements for 15 days.

The rheological properties of the hydrogels were studied in a HAAKE MARS III controlled stress rheometer using parallel serrated plates with a diameter of 20 mm and a gap of 0.25 mm at 20 ± 0.5 °C. The hydrogels were formed in a 3D printed mold with 8 mm diameter and 1 mm height, with a total volume of 50 μ l. A shear stress sweep was carried out at constant frequency (1 Hz) to determine the linear viscoelastic region, where no variation of G' (storage modulus) and G'' (loss modulus) was observed. The viscoelastic properties (G' and G'') of the hydrogels were determined by frequency sweep experiments (0.01-100 Hz) at the constant stress value within the linear viscoelastic region (Figure S4). A constant stress of 1 Pa was used in the frequency sweeps of 4-arm 2.5% and 4-arm 5% samples, and a constant stress of 0.5 Pa was used for 8-arm 2.5% sample. Before measurements, a thin layer of low-viscosity paraffin oil was used to cover the free surface of the rheometer plate to prevent evaporation of solvent. The assay was performed in duplicates.

Evidence of new interactions established between the hydrogel components was assessed by FTIR-ATR spectra (16 scans) of the hydrogels, recorded in the range 400-4000 cm^{-1} on a PerkinElmer FT-IR Spectrometer Spectrum Two, using the UATR Two module (L160-1742 tip, with a force gauge of 0 or close to 0).

The morphology of the hydrogels was characterized by scanning electron microscopy (SEM). Hydrogels were prepared as described previously with a total volume of 10 μ l over a glass slide. The sample was frozen at -20 °C and lyophilized. Samples were coated with 15 nm layer of iridium using a Quorum evaporator, and then analysed in a Carl Zeiss AURIGA CrossBeam FIB-SEM workstation.

2.2.4 Hydrogel biocompatibility

The biocompatibility of the hydrogel was assessed by indirect and direct toxicity tests, according to the guidelines of the International Organization for Standardization ^{39,40} and as previously described ²⁸.

For the indirect test, L929 mouse fibroblast cell line was seeded at a density of 80000 cell/cm² in a 24-well culture plate, corresponding to 160000 cells/well. The cells were covered with 0.5 ml of complete DMEM medium with 10% (v/v) of fetal bovine serum (FBS), 2 mM of glutamine and 1% (v/v) of a commercial mixture of antibiotics (Pen/Strep, 100 units/mL of penicillin, 100 µg/mL of streptomycin, and 0.025 µg/mL of Amphotericin B in sterile PBS), and incubated for 24 hours at 37 °C and 5% CO₂. The components necessary to form the 2.5 % (w/v) hydrogel (5% avidin and 5% PEG-[biotin]₄) were dissolved in 12.5 µl of PBS and maintained under UV light for 15 minutes. Afterwards, the hydrogel was formed in a well in a separated culture plate and incubated with 0.5 ml of Pen/Strep for 30 minutes. Simultaneously, a piece of a latex glove was cut and sterilized with 0.5 ml Pen/Strep solution. The supernatant was removed, the materials were washed twice with 0.5 ml sterile PBS and covered with 0.5 ml cell culture medium. The following day, cells were observed under an inverted optical microscope to confirm the formation of a monolayer of cells at around 80% of confluency. The medium covering the cells was replaced by the medium maintained overnight with the materials. Cells were then incubated for an additional 24 hours at 37 °C and 5% CO₂. The next day, the morphology of the cells was checked under an inverted optical microscope. Then, the MTT solution was prepared as followed: (a) a 5 mg 3-(4,5-dimethylthiazol-2-yl)-2,5-diphenyltetrazolium bromide) / ml sterile PBS stock solution was prepared by mixing the solution using a vortex until complete dissolution; (b) the solution was diluted to 1 mg/ml in PBS. The cell medium was

removed, and the wells were washed with 0.5 ml of PBS. A volume of 0.3 ml of 1 mg/ml MTT solution was added to each well and was incubated for 2 hours at 37 °C. Afterwards, the MTT solution was removed from the plate and 1 ml of MTT solvent (10% (v/v) of isopropanol in 10 M HCl) was added to each well. The plates were agitated for 5 minutes and a volume aliquot of 0.2 ml was transferred to a transparent 96-well plate. The absorbance was quantified at 570 nm using a plate reader (Tecan). Using the control cells maintained in culture medium only for reference, total cell viability was calculated according to Equation 1.

$$Viability = \frac{Absorbance (sample)}{Absorbance (control)} \% \quad \text{Equation 1}$$

For the direct biocompatibility test, the components necessary to form the hydrogel (5% avidin and 5% PEG-[biotin]₄) were dissolved in 12.5 µl of PBS and put under UV light for 15 minutes. The same sterilization procedure was done on a piece of latex glove. L929 fibroblasts cell line was seeded at a density of 80000 cell/cm² in a 24-well culture plate, corresponding to 160000 cells/well. The cells were covered with 0.5 ml of DMEM medium with 10% fetal bovine serum and incubated for 24 hours at 37 °C and 5% CO₂. The following day, the cells were observed under an inverted optical microscope to confirm the formation of a monolayer (around or more than 80% confluence). The media covering the cells was removed and discarded. Afterwards the latex glove was put on top of the cells. In case of the hydrogel, both solutions were simultaneously pipetted on top of the monolayer. The cells and materials were covered with 0.5 ml cell media and were incubated for 24

hours at 37 °C and 5%. The next day, the morphology and distribution of the cells near the materials were checked under the microscope.

2.2.5 Stem cell encapsulation and differentiation

Gibco™ human induced pluripotent stem cell (hiPSC) line (from Thermo Fisher Scientific) was used for the experimental procedures. This is a viral-integration-free hiPSC line generated using human cord blood-derived CD34+ progenitors with seven episomally expressed factors (Oct4, Sox2, Klf4, Myc, Nanog, Lin28, and SV40T). The hiPSCs were routinely cultured on Matrigel-coated plates in TeSR™2 medium in a humidified 5%CO₂ incubator at 37°C. The medium was daily refreshed and when cells reached 80% confluence, the EDTA method was used to passaged cells at a split ratio of 1:4⁴¹.

Prior to cell aggregation, cells were incubated with culture medium supplemented with 10 μM of Rho kinase inhibitor (ROCKi, Y-27632) (STEMCELL Technologies™) at 37°C for 1 h. After culture medium removal, cells were washed with PBS and then incubated with Accutase® solution (Sigma-Aldrich®/ Merck) at 37°C for 7 min for single-cell formation. Cells were flushed with Accutase® solution and collected to a centrifuge tube with culture medium, for inactivation of enzymatic digestion, and centrifuged at 200g for 3 min. Cell pellet was resuspended in culture medium supplemented with ROCKi (10 μM) followed by seeding onto AggreWell™400 plate (STEMCELL Technologies™) with a cell density of 1.5x10⁶ cells/well (1.3x10³ cells/microwell) for a final volume of 1.5 mL/well. Before seeding, the AggreWell™400 plate was centrifuged at 2700g for 5 min and after seeding at 300g for 3 min. Cells settle by gravitation and self-aggregate to form 3D aggregates. Cells were kept in a CO₂ incubator at 37°C, 5% CO₂ and 20% O₂, and after the first 24h culture medium was changed daily without ROCKi. On day 2, cells were encapsulated in the

avidin/PEG-[biotin]₄ hydrogel. Before the encapsulation process, avidin is diluted in 21.75 μL of TeSRTM2 medium with a final concentration of 10% (v/v). The same procedure is performed for the PEG-[biotin]₄. Afterwards, the 3D aggregates are retrieved from the aggregewell and added to a falcon tube. The aggregates settled to the bottom and the supernatant was discarded. Fresh media was added (43.5 μL) to resuspend the aggregates. This volume was then divided in equal parts by the components A and B, which were diluted to 5% (v/v). In a 24-well plate, 12.5 μL of A and B were added to a well to allow the physical gelation of the hydrogel by self-assembly. This procedure was done using at least three replicates.

LIVE/DEAD[®] viability/cytotoxicity Kit (Thermo Fisher Scientific) was used to assess the viability of expanded hiPSCs. Before the encapsulation process, the aggregates were incubated for 20 minutes with Calcein AM solution according to the manufacturer's instructions. The aggregates were then encapsulated, and cell viability was assessed through fluorescence microscopy. On day 5 of expansion, the encapsulated aggregates were recovered, and the same Calcein AM staining procedure was repeated to assess whether cells would maintain their viability. Non-encapsulated aggregates were used as controls. At least three replicates were used to measure the fluorescence intensities from the images using Fiji ImageJ. Two-way ANOVA tests were used to assess statistical significance between conditions.

After 3 days of encapsulation cells were harvested and replated on Matrigel-coated plates. In parallel assays, aggregates encapsulated for 2 days were induced to differentiate. To promote neural differentiation, TeSRTM2 culture medium was replaced daily by Essential 6TM medium supplemented with 1:200 (v/v) of PenStrep for a period of 14 days. Afterwards, part of the encapsulated aggregates was harvested, and part was replated onto

laminin-coated plates for immunocytochemistry assays. In both cases, cells were fixed with 4% (w/v) of paraformaldehyde (PFA). Non-encapsulated aggregates were replated in the same manner and used as controls. For immunocytochemistry assays, the protocol is described elsewhere⁴². Primary antibodies used for the immunocytochemistry assay comprised the pluripotency markers OCT4 (1:200; Millipore), SOX2 (1:200; R&D Systems) and the differentiation markers PAX6 (1:400, Covance), NESTIN (1:500, R&D Systems) and ZO-1 (1:200, Novex). The secondary antibodies included goat anti-mouse IgG Alexa Fluor– 488 or 546 (1:500), and goat anti-rabbit IgG Alexa Fluor 546 (1:500) from Invitrogen. Nuclei was counterstained using DAPI. In the case of OCT4 and SOX2 staining, at least three replicates were used to measure the fluorescence intensities from the images using Fiji ImageJ. The percentage of cells expressing SOX2 and OCT4 could be calculated based on the quantification of the mean fluorescence intensity in the red channel, that corresponds to the cells expressing the pluripotency markers OCT4 and SOX2, and of the blue channel (all cell nuclei counterstained with DAPI).

3. Results and Discussion

3.1 Selection of multivalent PEG-biotin for hydrogel formation

In multicomponent protein hydrogels, as affinity-triggered hydrogels, gel assembly is promoted by the crosslinking between the multivalent components. This bottom-up approach takes advantage of the selective molecular recognition between known affinity pairs ligand-receptor, in combination with multivalent display approaches to guide their autonomous self-assembly into robust nano-, micro- and macrostructures. The simplest approach to generate multivalency includes the employment of natural multimeric proteins and their cognate ligands. In particular, avidin is a natural tetrameric protein with four

biotin-binding sites. Biotin is a water-soluble vitamin acting as a cofactor in multiple metabolic pathways (**Figure 1 A, B**). Avidin can be biotechnologically produced at high yields⁴³, and biotin is also widely available. This affinity pair is extremely interesting due to the high binding constants reported, and due to the wide variety of avidin variants and avidin-binding peptides which further enlarge the tunability of the system^{44,45}.

In this work, avidin was employed as the multimeric protein, and biotin cadaverin was conjugated in high yields (higher than 95%) to multi-arm 20 kDa PEG molecules (linear, 4-arm and 8-arm) to generate multivalency. Branched PEG polymers are particularly suited to hydrogel formation – PEG polymers are hydrophilic, chemically well defined, and available at a wide range of molecular weights and chemistries. The success of PEG functionalization was confirmed by ICP and further observed by FTIR-ATR analysis of the PEG oligomers (Figure S1).

The assembly of affinity-triggered hydrogels implies the existence of molecular recognition and binding between each hydrogel component. The binding constant between free avidin and free biotin is well reported³⁴, but it is known that after immobilizing the ligand or the receptor into soluble or insoluble polymers in matrices, the binding constants are altered, as the matrix itself plays a role in the molecular recognition event by generating a local microenvironment^{28,46–48}. Furthermore, the availability of the affinity pair elements to bind is modified, and several partitioning and stereo hindrance effects may occur.

In this work, biotin was conjugated to PEG oligomers (20 kDa) with distinct multimerization (Figure 1A). Microscale Thermophoresis (MST) (Figure S2) was used to determine the binding constants between avidin and each biotin-PEG oligomer. It was observed that the PEG-[biotin]₄ presented the highest affinity constant ($1.6 \times 10^8 \text{ M}^{-1}$). When decreasing (PEG-[biotin]₂) or increasing (PEG-[biotin]₈) the biotin multivalency, the

affinity constant decreased one order of magnitude presenting K_a values of $6.3 \times 10^7 \text{ M}^{-1}$ and $7.1 \times 10^7 \text{ M}^{-1}$, respectively (Figure 2A). These results show the influence of PEG chains flexibility and steric hindrance in promoting the interaction between biotin and avidin. It also elucidates that the 4-arm PEG displays the most appropriate multivalency and geometry to display free biotin molecules and promote the interaction with tetrameric avidin.

In fact, when mixing avidin and PEG-[biotin]₄ (equal mass amounts) a hydrogel was instantaneously formed. Each 4-arm PEG molecule functionalized with biotin can bind to more than one molecule of the tetrameric avidin, which allows the crosslinking of biotinylated PEG oligomers via avidin-biotin interactions and, consequently, the formation of a network. Different concentrations were tested to assess the critical gelation concentration for the avidin/PEG-[biotin]₄ system: 0.1%, 0.5%, 1%, 2.5%, 5% and 10% (w/v) (Figure 1C). An increase of concentration resulted in an increase of viscosity of the mixture. Above 2.5%, a physically crosslinked network was instantaneously formed, and a self-supporting hydrogel was observed by the vial inversion test. Below 2.5%, the solution remained viscous. When PEG-[biotin]₈ was mixed with avidin at the same concentration (2.5%), a self-supporting hydrogel was also formed. When linear biotinylated PEG was mixed with avidin at 2.5%, no hydrogel was formed. Liu and colleagues³⁷ used 1.5 kDa linear biotin-conjugated PEG and were able to observe the formation of a hydrogel; however hydrogels were obtained at a much higher concentration (13.3%). As such, in our work, the avidin/PEG-[biotin]₂ system was no longer studied.

Free biotin lacks the physical hindrance of biotin conjugated to a large PEG polymer, being able to occupy the binding pockets of avidin more easily, which leads to hydrogel surface erosion. When adding free biotin (2 mg/ml) to 2.5% avidin/PEG-[biotin]₄ hydrogels, an

increase of erosion is observed, until the hydrogel completely dissolves into solution after 16 days (Figure 1D and 1E). The control avidin/PEG-[biotin]₄ hydrogel in the presence of PBS alone presents a 15% erosion after 20 days. Previous authors also observed faster hydrogel dissolution in the presence of non-conjugated biotin^{34,38}. The avidin/PEG-[biotin]₄ hydrogel was also characterized by ATR-FTIR and it is possible to observe interactions between avidin and biotin that contribute for hydrogel formation (Figure S3).

Taken together, our data further confirms that the driving force for hydrogel formation is the affinity between avidin and biotin. In addition, it establishes that both affinity of the avidin-PEG system and multivalency are critical parameters to provide enough physical interactions between the two components to yield a macroscopic self-supportive gel.

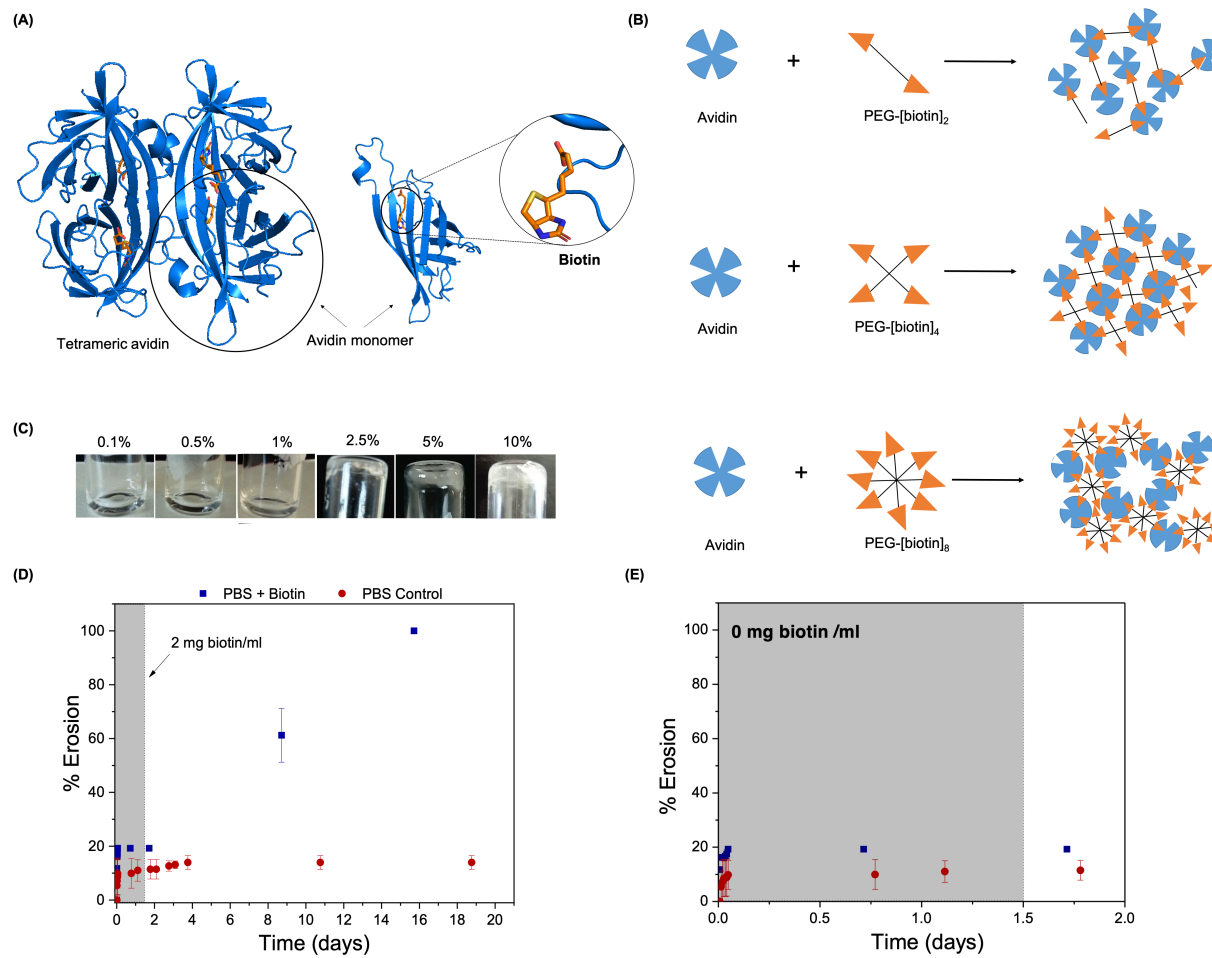


Figure 1 – (A) Structure of tetrameric avidin, detailing the interaction between one unit of avidin with the ligand biotin (2AVI.pdb) (B) Schematic representation of an affinity-triggered hydrogel self-assembly based on the affinity pair avidin and biotin and their corresponding affinity constant, as determined by microscale thermophoresis. (C) Images of the mixture between biotinylated 4-arm

PEG and free avidin at different concentrations: 0.1%, 0.5%, 1%, 2.5%, 5% and 10% (w/v). (D) Erosion profile of avidin/PEG-[biotin]₄ hydrogels in the presence of PBS (15% after 20 days) or PBS containing 2 mg biotin/ml (100% after 16 days) (E) Erosion profile at beginning before adding 2mg/ml biotin (stdev correspond to 3 replicates).

3.2 Properties of avidin/PEG-Biotin hydrogels

Considering that only avidin/PEG-[biotin]₄ and avidin/PEG-[biotin]₈ systems yielded self-supported gels, these materials were further characterized. The mechanical properties and erosion profile of the gels were considered as a function of the measured affinity constant (Figure 2 A).

When maintaining the concentration of the hydrogel components constant (2.5% (w/v)), the multivalency effect was studied. The affinity between avidin/PEG-[biotin]₈ was determined as $7.1 \times 10^7 \text{ M}^{-1}$, an order of magnitude lower than that for the avidin/PEG-[biotin]₄ system. The avidin/PEG-[biotin]₈ hydrogel was visibly weaker than the avidin/PEG-[biotin]₄ hydrogel, presenting a lower mechanical stability ($G' = 0.9 \text{ Pa}$). This also translated into a complete gel erosion after 5 hours (figure 2A, figure 2B). Physical hydrogels usually degrade by a surface-erosion model, as the crosslinks are maintained by labile dynamic affinity interactions³⁴. As avidin has four biotin binding pockets per molecule, the PEG-[biotin]₄ allowed the formation of a more precise, effective and stable network than PEG-[biotin]₈. On the other hand, gelation time can influence the observed properties. Other authors described an increased gelation time for PEG hydrogel with 8-arm versus 4-arm (6 hours and 2 hours, respectively)⁴⁹. In our case this effect was not relevant as gelation occurred instantly.

The effect of concentration (2.5% and 5% (w/v)) was further studied for the avidin/PEG-[biotin]₄ hydrogels. Both avidin/PEG-[biotin]₄ hydrogels were robust, and only 15% erosion was observed after three months (figure 2A-2B). In fact, the high affinity between avidin and biotin led to the formation of a non-degradable hydrogel over three months. The system described was far more stable over time than other avidin/linear PEG-biotin hydrogels described in the literature, which were completely degraded after 5 days, even at concentrations as high as 14% (w/v)³⁴. In terms of mechanical properties, the 2.5% avidin/PEG-[biotin]₄ hydrogels were weaker (average $G' = 1.3 \text{ Pa}$ in the plateau) than the 5% hydrogels (average $G' = 8.9 \text{ Pa}$ in the plateau), due to the lower mass content which results in

less crosslinks between the components (figure 2A). The storage modulus value is comparable to some reported multimeric protein/PEG-conjugated affinity-triggered hydrogels (e.g. TIP1 (trimeric)/PEG-TIP1 binding peptides hydrogels^{22,23}). However, it was not possible to compare to other avidin/biotin affinity hydrogels, as the mechanical properties were not reported. The reported avidin/PEG-[biotin]₄ hydrogels are weak hydrogels, which assembly occurs spontaneously and under mild conditions, which makes them advantageous to be explored for *in vitro* expansion of stem cells and cell therapy.

Due to a higher affinity constant, stability over time and better mechanical performance, the avidin/PEG-[biotin]₄ was chosen to proceed with this work. The morphology and microstructure of 2.5% avidin/PEG-[biotin]₄ hydrogels were analysed by SEM (Figure S5) and presented a very porous inner structure displaying large pores with $11.2 \pm 0.2 \mu\text{m}$ in diameter.

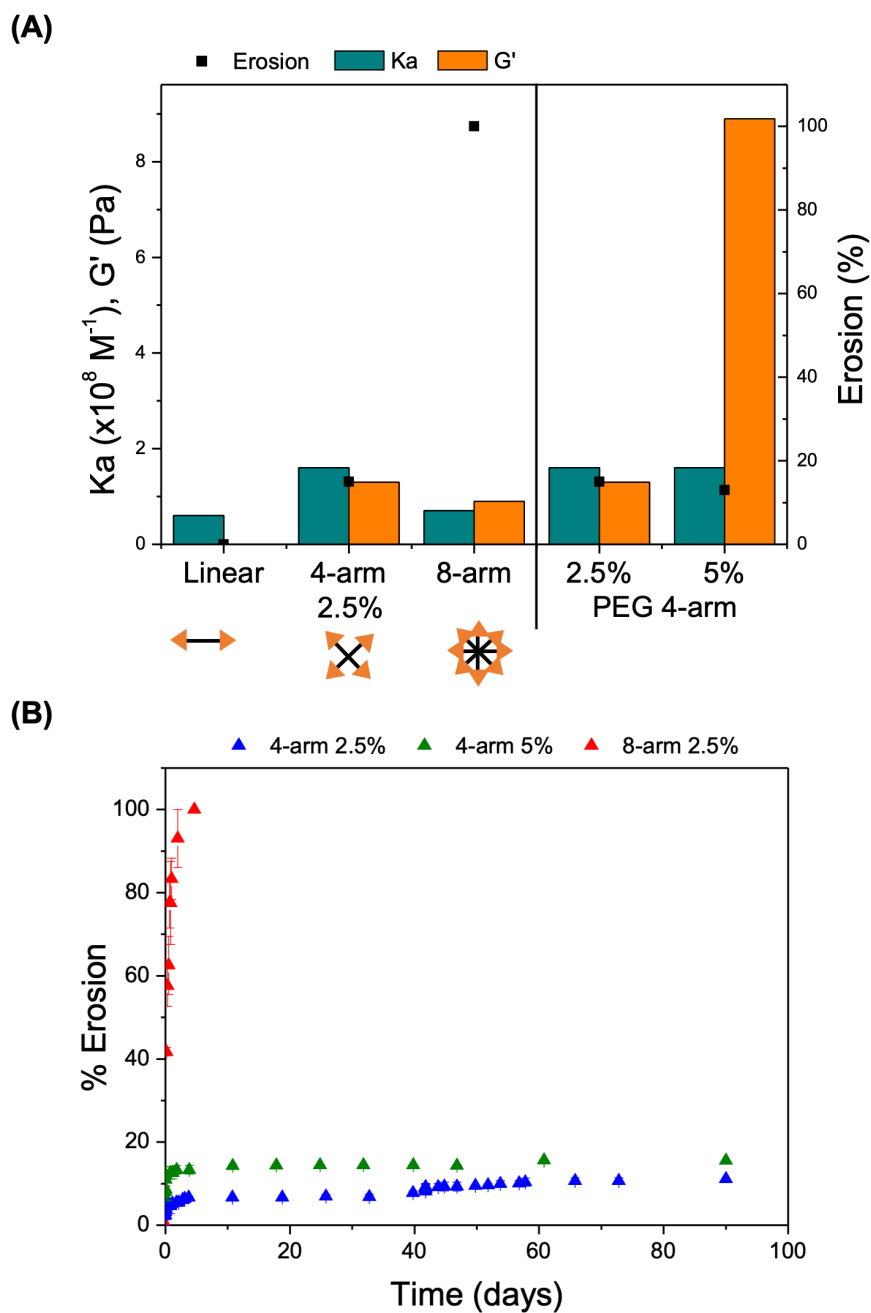


Figure 2 – Properties of avidin-biotin hydrogels. (A) Comparison of the affinity constant (Ka), erosion percentage (at 5 hours) and storage modulus (G') for the avidin/PEG-[biotin] hydrogels. Erosion profiles (B) of avidin/biotin hydrogels in terms of concentration (2.5% versus 5%) and multivalency (4-arm versus 8-arm PEG at 2.5%). (stdev correspond to 2 replicates)

3.3 Stem cell encapsulation, expansion and neural commitment

Encapsulation is a very common application for affinity-triggered hydrogels, which have been explored for the encapsulation of chondrocytes²³, mesenchymal stem cells^{22,50}, PC-12 cells, murine adult neural stem cells²⁵, human umbilical vein embryonic cells^{25,29} and adipose-derived stem cells^{24,27}, with high cell viability after different time lengths. However only one other avidin/biotin hydrogel has been used for cell encapsulation, specifically human mesenchymal stromal cells³⁴. In this context, to the best of our knowledge, we advance for the first time an affinity-triggered hydrogel capable to support the encapsulation, expansion and differentiation of human pluripotent stem cells. In fact, the encapsulation of pluripotent stem cell derivatives is a promising approach for cell replacement therapies.

The cell biocompatibility of 2.5% avidin/PEG-[biotin]₄ hydrogels was first assessed (Figure S6). Fibroblasts were chosen as the target cells, due to their robustness⁵¹. Two types of toxicity were studied: indirect and direct. The indirect toxicity studied if the material leaks any toxic by-products into the medium. The supernatant containing the released by-products was used to culture a fibroblasts monolayer and their viability was assessed by the MTT assay (Figure S6A). Fibroblasts showed 100% viability compared to the positive control. This was expected, as all hydrogel components are biocompatible (avidin, biotin and PEG¹⁰) and low erosion was observed for longer times than the one tested in this assay. Other avidin/PEG-[biotin] hydrogels also allowed for high cell viability after the encapsulation of human mesenchymal stromal cells³⁴.

In comparison, the negative control (supernatant containing by-products of latex) showed low cell viability (11.8%). This toxic effect has been reported before⁵², with higher toxicity after extraction with serum-free media and culture media with serum compared to distilled water and saline solution. Natural rubber latex contains Hevb1 and Hevb3⁵² and other chemicals that are added during the manufacturing process⁵³, and are the principal components responsible for latex hyper sensibility. In this assay, they are responsible for cell toxicity.

Direct toxicity studied if the material had toxic effects on an already formed monolayer of cells. Fibroblasts cultured in contact with the hydrogel grew in a compact monolayer, with no morphology alterations (typical elongated shape) (Figure S6B). Furthermore, as the hydrogel is translucent, it is possible to observe well-shaped cells growing underneath the hydrogel, suggesting that the hydrogel does not prevent oxygen and nutrients to reach the cells. In comparison, cells cultured in contact with latex, died in the proximity of the material and adopted a round shape (Figure S6C).

After showing that the hydrogel was biocompatible, we next aimed to encapsulate hiPSC aggregates using the avidin/PEG-[biotin]₄ hydrogel and assess its impact on the maintenance of a pluripotent phenotype (**Figure 3 A**). Pluripotent stem cell encapsulation has been used to promote cell expansion and differentiation into specific phenotypes, and is an ideal solution for cell replacement therapies⁴⁻⁶. Stem cell encapsulation is used to increase local cell densities, decrease cell losses and increase cell survival.

We started by first comparing encapsulation of single cells vs 3D aggregates for 5 days of expansion in xeno-free conditions. Our preliminary experiments demonstrated that even with the addition of ROCK inhibitor, single cells rapidly lost viability when compared to the encapsulated aggregates (data not shown). Since the hydrogel does not contain any ECM components, we hypothesised that there is a lack of structural support, which is surpassed by using the 3D approach in our system. As a result, a density of 1.3×10^3 cells/microwell was used to produce aggregates with a controlled size diameter. In Figure 3B, it is possible to observe the formation of the aggregates from day 0 to day 2 of culture using the xeno-free culture medium (TeSR™2). Before the encapsulation process, cells were incubated with a solution of calcein AM diluted in TeSR2 culture medium. This step was performed to assess the viability through fluorescence microscopy. In Figure 3C, it is possible to observe the result before and after the encapsulation (day 2), which demonstrates the viability of cells

throughout the process. Also, encapsulated aggregates were comparable to non-encapsulated controls (Figure S7 A). On day 5, the same procedure was repeated to demonstrate that cells would maintain their viability throughout 3 days of encapsulation. The viability is demonstrated by the conversion of the non-fluorescent calcein AM into a green fluorescent probe as the result of acetoxymethyl ester hydrolysis by intracellular esterases (Figure 3C). Therefore, it is possible to conclude that aggregates did not experience problems regarding nutrient and gas diffusion inside the hydrogel throughout the expansion period. More importantly, cells were able to grow inside the hydrogel, as it is possible to observe and quantify from the fluorescent microscopy images (Figure 3C and S7 B). Importantly, the encapsulation and expansion of hiPSC aggregates in our system was performed in entirely defined, xeno-free conditions. One of the important design criteria to develop functional and clinically relevant cell culture platforms is the absence of serum or serum placements, which may contain xenogeneic factors^{4,54}. This decreases the potential of immunogenic risk in the translation to a clinical setting.

After 3 days of expansion, the aggregates were mechanically harvested from the hydrogel and replated onto Matrigel-coated plates to perform immunocytochemistry assays. In Figure 3D and Figure 3E, it is possible to observe that the replated cells were able to grow as colonies with typical morphology of undifferentiated pluripotent stem cells. Moreover, cells were positively stained for two intracellular pluripotency markers, OCT4 and SOX2, which are essential transcription factors used for somatic cell reprogramming towards an embryonic-like state⁵⁵. This was comparable to the non-encapsulated controls (Figure S8A). Together with NANOG, SOX2 and OCT4 are part of a complex regulatory network that control gene expression for potency maintenance as well as embryonic development⁵⁶. For instance, OCT4 was shown to be essential for the formation of the inner cell mass of the blastocyst⁵⁷. Downregulation of OCT4 can induce pluripotent stem cells to differentiated into the trophoblast, and to a greater extend towards primitive endoderm and mesoderm lineages⁵⁸. In

the case of SOX2, the expression of this marker is initiated in the morula stages and it is essential for neural lineage commitment, where it promotes the neuroectodermal fate by suppressing mesodermal regulator genes⁵⁹. Moreover, depletion or over expression of SOX2 can induce human pluripotent stem cells to differentiate towards the trophectoderm⁶⁰. Therefore, by the quantification of the expression of these two transcription factors (Figure S8B), it is possible to conclude that hiPSCs maintained their undifferentiated state while being cultured under xeno-free conditions.

To further demonstrate the usefulness of our encapsulation system, we tested if cells could differentiate inside the hydrogel, and to that end we induced neural differentiation after the encapsulation stage (Figure 3F). On day 14 of neural commitment, part of the aggregates was harvested from the hydrogel for immunocytochemistry analysis. Similarly, the rest of the aggregates were collected and replated in laminin-coated plates to assess the presence of hiPSC-derived neural progenitor cells (hiPSC-NP). From Figure 3G-H and Figure 3I-J, it is possible to observe that both aggregates and replated cells positively co-stained for PAX6 and Nestin, which comprise a transcription factor for neuroectoderm specification and an intermediate filament protein expressed in undifferentiated cells from the central nervous system, respectively^{61,62}. Moreover, immunocytochemistry analysis demonstrated the presence of SOX2 and apical ZO1 markers, further revealing polarized structures within the aggregate, which are consistent with the formation of neuro-epithelial rosettes that recapitulate the neural tube formation *in vivo*^{63,64}. These structures were also observed in the replated cells, which confirms the substantial maturation of hiPSC-NP⁶⁵. Furthermore, we could not discern differences in rosette formation after replating encapsulated aggregates or non-encapsulated (control) aggregates following neural commitment (Figure S9). Only one example of an affinity-triggered hydrogel has reported to allow the self-renew and differentiation of neuronal-like PC-12 cells and dissociated murine adult neural stem cells, as cells adopted typical neural morphologies after differentiation²⁵. By comparison, the results

obtained in this work show that the avidin/PEG[biotin]₄ hydrogel can be used as a support material for encapsulation, expansion and neural commitment of hiPSCs and, most importantly, we demonstrate for the first time that an affinity-triggered hydrogel can be successfully used to generate phenotypically mature neural progenitors under xeno-free conditions. This constitutes an important first step towards the development of cell replacement therapies, where such hydrogels could support and guide the effective integration of cells at the site of injury.

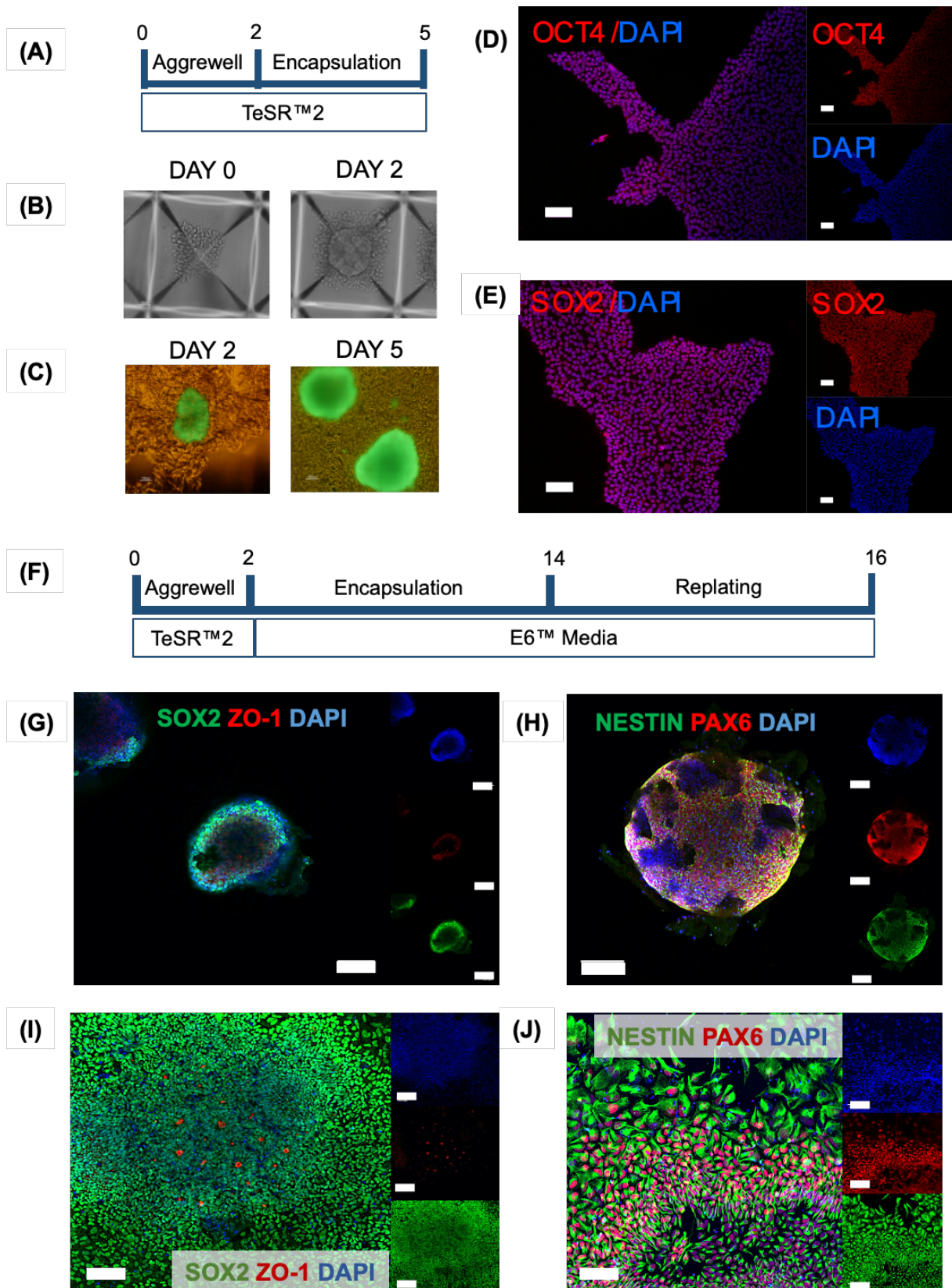


Figure 3 - hiPSC encapsulated in avidin/PEG-[biotin]₄ hydrogels. (A-E) Pluripotency and viability assessment of encapsulated cells using xeno-free TeSR2 expansion medium. (A) Graphical representation of the culture period of hiPSC aggregates encapsulated in the hydrogel. (B-C) Aggregates were formed with an initial cell density of 1.250×10^3 cells/aggregate. After 2 days of expansion in microwells, aggregates were removed and

encapsulated in the Avidin-Biotin Affinity Hydrogel. (C) Brightfield microscopy image with the green fluorescence channel open to depict the 3D aggregates encapsulated in the hydrogel. Calcein AM viability assay was performed at day 2 and day 5 of encapsulation. The fluorescence channel is used to detect green fluorescence from the metabolized calcein AM, and corresponds to live cells. (D-E) After 5 days of encapsulation cells were harvested and replated on Matrigel-coated plates to assess pluripotency maintenance. Immunocytochemistry was performed on pluripotency intracellular markers, namely (D) OCT4 and (E) SOX2. Nuclei were counterstained with DAPI. (F-J) Neural differentiation of encapsulated cells using xeno-free Essential 6 medium. (F) Graphical representation of the neural differentiation protocol. hiPSC aggregates were formed as in the previous case. After 2 days, aggregates were encapsulated in the hydrogel and cultured with E6 medium to induce neural differentiation. After 14 days, aggregates were harvested from the hydrogel and replated on laminin-coated plates. (G-H) Immunocytochemistry of hiPSC harvested aggregates for neural differentiation markers: SOX2 (green) co-marked with ZO-1 (red) and PAX6 (red) co-marked with NESTIN (green). DAPI (blue) was used to counterstain nuclei. (I-J) Immunocytochemistry of replated aggregates for neural differentiation markers: SOX2 (green) co-marked with ZO-1 (red) and PAX6 (red) co-marked with NESTIN (green). DAPI (blue) was used to counterstain nuclei.

4. Conclusions

Affinity-triggered hydrogels have shown several applications in tissue engineering and drug delivery. Affinity interactions can be rationally explored to develop tailored-made hydrogels, exposing predictable design rules which correlate natural and strategic multivalency. In this work, PEG molecules with different multivalency were conjugated to biotin, and further mixed with avidin to yield hydrogels with different characteristics. The hydrogel avidin/PEG-[biotin]₄ was proven to be cell-compatible and was successfully used to encapsulate pluripotent stem cells and to induce neural lineage in a xeno-free medium. The results showed that the developed hydrogel has the potential to increase local cell densities, maintain cell viability, and support human iPSC expansion and differentiation. The affinity-triggered hydrogel was able to encapsulate and sustain for the first time the commitment of pluripotent stem cells into phenotypically mature neural progenitors under xeno-free conditions. This technology could be further translated into a broader application in neural cell replacement therapies, like in Parkinson's disease for example. Such an approach has allowed the design of multicomponent hydrogels inspired in Nature and Biology, that have proven to be important tools for the non-invasive and mild cell encapsulation, a requisite for tissue and cell therapies.

Acknowledgments

This work was financed by FCT/MEC (PTDC/BII-BIO/28878/2017, UIDB/04378/2020, UID/QUI/50006/2019 and UID/AGR/04129/2019) and co-financed by the ERDF under the PT2020 Partnership Agreement (POCI-01-0145-FEDER-007728 & LISBOA-01-0145-FEDER-028878).

The authors thank FCT/MEC for the research fellowship SFRH/BPD/97585/2013 for A.S.P, and PD/BD/105871/2014 for C.S.M.F and PD/BD/135524/2018 for A.L.R. The authors

would like to acknowledge the Laboratório de Análises (FCT-NOVA) for the ICP analysis and the BioLab (FCT-NOVA) for the MST assays.

Author contributions

CSFM, TGF, ASP, ACAR designed the experiments and wrote the manuscript. CSFM performed the experiments CSFF, ALR and TGF performed the cell-based assays. CSFM, VA and ASP performed the rheological experiments. All the authors analysed the data.

Declaration of interests

The authors declare no conflict of interests.

Supporting information

Characterization of multivalent PEG-biotin for hydrogel formation (FTIR-ATR; microscale thermophoresis); Properties of avidin/PEG-Biotin hydrogels (FTIR-ATR; rheology and SEM analysis); Stem cell encapsulation, expansion and neural commitment (Hydrogel biocompatibility); Analysis of total Calcein intensity for encapsulated aggregates; Pluripotency assessment of non-encapsulated aggregates; Neural differentiation of non-encapsulated aggregates replated at day 12 on Matrigel-coated plates.

References

- (1) Prince, E.; Kumacheva, E. Design and Applications of Man-Made Biomimetic Fibrillar Hydrogels. *Nat. Rev. Mater.* **19AD**, 4, 99–115.
- (2) Hussey, G. S.; Dziki, J. L.; Badylak, S. F. Extracellular Matrix-Based Materials for Regenerative Medicine. *Nat. Rev. Mater.* **2018**, 3, 159–173.
- (3) Custódio, C. A.; Reis, R. L.; Mano, J. F. Engineering Biomolecular Microenvironments for Cell Instructive Biomaterials. *Adv. Healthc. Mater.* **2014**, 3 (6), 797–810.
- (4) Adil, M. M.; Rodrigues, G. M. C.; Kulkarni, R. U.; Rao, A. T.; Chernavsky, N. E.;

- Miller, E. W.; Schaffer, D. V. Efficient Generation of hPSC-Derived Midbrain Dopaminergic Neurons in a Fully Defined, Scalable, 3D Biomaterial Platform. *Sci. Rep.* **2017**, *7*, 40573.
- (5) Lin, H.; Li, Q.; Leia, Y. An Integrated Miniature Bioprocessing for Personalized Human Induced Pluripotent Stem Cell Expansion and Differentiation into Neural Stem Cells. *Sci. Rep.* **2017**, *7*, 40191–40198.
- (6) Lei, Y.; Schaffer, D. V. A Fully Defined and Scalable 3D Culture System for Human Pluripotent Stem Cell Expansion and Differentiation. *Proc. Natl. Acad. Sci.* **2013**, *110* (52), E5039–E5048.
- (7) Adil, M. M.; Schaffer, D. V. Engineered Hydrogels Increase the Post-Transplantation Survival of Encapsulated hESC-Derived Midbrain Dopaminergic Neurons. *Biomaterials* **2017**, *136*, 1–11.
- (8) Cai, L.; Heilshorn, S. C. Designing ECM-Mimetic Materials Using Protein Engineering. *Acta Biomater.* **2014**, *10* (4), 1751–1760.
- (9) Chai, C.; Leong, K. W. Biomaterials Approach to Expand and Direct Differentiation of Stem Cells. *Mol. Ther.* **2007**, *15* (3), 467–480.
- (10) Jonker, A. M.; Löwik, D. W. P. M.; Van Hest, J. C. M. Peptide- and Protein-Based Hydrogels. *Chem. Mater.* **2012**, *24* (5), 759–773.
- (11) Dawson, E.; Mapili, G.; Erickson, K.; Taqvi, S.; Roy, K. Biomaterials for Stem Cell Differentiation. *Adv. Drug Deliv. Rev.* **2008**, *60* (2), 215–228.
- (12) Koetting, M. C.; Peters, J. T.; Steichen, S. D.; Peppas, N. A. Stimulus-Responsive Hydrogels: Theory, Modern Advances, and Applications. *Mater. Sci. Eng. R* **2015**, *93*, 1–49.
- (13) Edalat, F.; Bae, H.; Manoucheri, S.; Cha, J. M.; Khademhosseini, A. Engineering Approaches Toward Deconstructing and Controlling the Stem Cell Environment. *Annu. Biomed. Eng.* **2012**, *40* (6), 1301–1315.

- (14) Sengupta, D.; Heilshorn, S. C. Protein-Engineered Biomaterials: Highly Tunable Tissue Engineering Scaffolds. *Tissue Eng. Part B. Rev.* **2010**, *16* (3), 285–293.
- (15) Hinderer, S.; Layland, S. L.; Schenke-Layland, K. ECM and ECM-like Materials - Biomaterials for Applications in Regenerative Medicine and Cancer Therapy. *Adv. Drug Deliv. Rev.* **2016**, *97*, 260–269.
- (16) Huang, G.; Li, F.; Zhao, X.; Ma, Y.; Li, Y.; Lin, M.; Jin, G.; Lu, T. J.; Genin, G. M.; Xu, F. Functional and Biomimetic Materials for Engineering of the Three-Dimensional Cell Microenvironment. *Chem. Rev.* **2017**, *117* (20), 12764–12850.
- (17) Lutolf, M. P.; Hubbell, J. A. Synthetic Biomaterials as Instructive Extracellular Microenvironments for Morphogenesis in Tissue Engineering. *Nat. Biotechnol.* **2005**, *23* (1), 47–55.
- (18) Goor, O. J.; Hendrikse, S. I.; Dankers, P. Y.; Meijer, E. From Supramolecular Polymers to Multi-Component Biomaterials. *Chem. Soc. Rev.* **2017**, *46*, 6621–6637.
- (19) Ramakers, B. E. I.; van Hest, J. C. M.; Löwik, D. W. P. M. Molecular Tools for the Construction of Peptide-Based Materials. *Chem. Soc. Rev.* **2014**, *43* (8), 2743–2756.
- (20) Kopeček, J.; Yang, J. Smart Self-Assembled Hybrid Hydrogel Biomaterials. *Angew. Chem. Int. Ed. Engl.* **2012**, *51* (30), 7396–7417.
- (21) Clegg, J.; Peppas, N. Molecular Recognition with Soft Biomaterials. *Soft Matter* **2020**, *16*, 856–869.
- (22) Wang, J.; Zhang, J.; Zhang, X.; Zhou, H. A Protein-Based Hydrogel for in Vitro Expansion of Mesenchymal Stem Cells. *PLoS One* **2013**, *8* (9), e75727.
- (23) Ito, F.; Usui, K.; Kawahara, D.; Suenaga, A.; Maki, T.; Kidoaki, S.; Suzuki, H.; Taiji, M.; Itoh, M.; Hayashizaki, Y.; Matsuda, T. Reversible Hydrogel Formation Driven by Protein-Peptide-Specific Interaction and Chondrocyte Entrapment. *Biomaterials* **2010**, *31* (1), 58–66.
- (24) Parisi-Amon, A.; Mulyasmita, W.; Chung, C.; Heilshorn, S. C. Protein-Engineered

- Injectable Hydrogel to Improve Retention of Transplanted Adipose-Derived Stem Cells. *Adv. Healthc. Mater.* **2013**, *2* (3), 428–432.
- (25) Wong, C. T. S.; Foo, P.; Seok, J.; Mulyasmita, W.; Parisi-amon, A.; Heilshorn, S. C. Two-Component Protein-Engineered Physical Hydrogels for Cell Encapsulation. *Proc. Natl. Acad. Sci.* **2009**, *106* (52), 22067–22072.
- (26) Mulyasmita, W.; Cai, L.; Dewi, R. E.; Jha, A.; Ullmann, S. D.; Luong, R. H.; Huang, N. F.; Heilshorn, S. C. Avidity-Controlled Hydrogels for Injectable Co-Delivery of Induced Pluripotent Stem Cell-Derived Endothelial Cells and Growth Factors. *J. Control. Release* **2014**, *191*, 71–81.
- (27) Cai, L.; Dewi, R. E.; Heilshorn, S. C. Injectable Hydrogels with in Situ Double Network Formation Enhance Retention of Transplanted Stem Cells. *Adv. Funct. Mater.* **2015**, *25* (9), 1344–1351.
- (28) Fernandes, C. S.; Pina, A. S.; Barbosa, A. J. M.; Padrão, I.; Duarte, F.; Teixeira, C. A. S.; Alves, V.; Gomes, P.; Fernandes, T. G.; Dias, A. M. G. C.; Roque, A.C.A. Affinity-Triggered Assemblies Based on a Designed Peptide-Peptide Affinity Pair. *Biotechnol. J.* **2019**, *14* (11), 1800559.
- (29) Ehrbar, M.; Schoenmakers, R.; Christen, E. H.; Fussenegger, M.; Weber, W. Drug-Sensing Hydrogels for the Inducible Release of Biopharmaceuticals. *Nat. Mater.* **2008**, *7* (10), 800–804.
- (30) Feng, Q.; Xu, J.; Zhang, K.; Yao, H.; Zheng, N.; Zheng, L.; Wang, J.; Wei, K.; Xiao, X.; Qin, L.; Bian, L. Dynamic and Cell-Infiltratable Hydrogels as Injectable Carrier of Therapeutic Cells and Drugs for Treating Challenging Bone Defects. *ACS Cent. Sci.* **2019**, *5*, 440–450.
- (31) Feng, Q.; Wei, K.; Lin, S.; Xu, Z.; Sun, Y.; Shi, P.; Li, G.; Bian, L. Mechanically Resilient , Injectable , and Bioadhesive Supramolecular Gelatin Hydrogels Crosslinked by Weak Host-Guest Interactions Assist Cell in Filtration and in Situ Tissue

- Regeneration. *Biomaterials* **2016**, *101*, 217–228.
- (32) Okesola, B. O.; Mata, A. Multicomponent Self-Assembly as a Tool to Harness New Properties from Peptides and Proteins in Material Design. *Chem. Soc. Rev.* **2018**, *47* (10), 3721–3736.
- (33) Wu, J.; Li, P.; Dong, C.; Jiang, H.; Xue, B.; Gao, X.; Qin, M.; Wang, W.; Chen, B.; Cao, Y. Rationally Designed Synthetic Protein Hydrogels with Predictable Mechanical Properties. *Nat. Commun.* **2018**, *9* (620), 1–11.
- (34) Thompson, M. S.; Tsurkan, M. V.; Chwalek, K.; Bornhauser, M.; Schlierf, M.; Werner, C.; Zhang, Y. Self-Assembling Hydrogels Crosslinked Solely by Receptor-Ligand Interactions: Tunability, Rationalization of Physical Properties, and 3D Cell Culture. *Chem. - A Eur. J.* **2015**, *21* (8), 3178–3182.
- (35) Barbucci, R.; Magnani, A.; Roncolini, C.; Silvestri, S. Antigen–antibody Recognition by Fourier Transform IR Spectroscopy/attenuated Total Reflection Studies: Biotin–avidin Complex as an Example. *Biopolymers* **1991**, *31* (7), 827–834.
- (36) Wilchek, M. My Life with Affinity. *Protein Sci.* **2004**, *13* (11), 3066–3070.
- (37) Liu, Y.; Liu, J.; Xu, J.; Feng, S.; Davis, T. P. Biodegradable PEG Hydrogels Cross-Linked Using Biotin-Avidin Interactions. *Aust. J. Chem.* **2010**, *63* (10), 1413–1417.
- (38) Cui, Y.; Li, Y.; Duan, Q.; Kakuchi, T. Preparation of Hyaluronic Acid Micro-Hydrogel by Biotin-Avidin-Specific Bonding for Doxorubicin-Targeted Delivery. *Appl. Biochem. Biotechnol.* **2013**, *169* (1), 239–249.
- (39) International Organization for Standardization - ISO. ISO 10993-12: Biological Evaluation of Medical Devices. In *Geneva: ISO*; 1996; p Part 12: Sample preparation and reference material.
- (40) International Organization for Standardization - ISO. ISO 10993-5: Biological Evaluation of Medical Devices. In *Geneva: ISO*; 1999; p part 5: Tests for cytotoxicity: In vitro methods.

- (41) Beers, J.; Gulbranson, D.; George, N.; Siniscalchi, L.; Jones, J.; Thompson, J.; Chen, G. Passaging and Colony Expansion of Human Pluripotent Stem Cells by Enzyme-Free Dissociation in Chemically Defined Culture Conditions. *Nat. Protoc.* **2012**, *7*, 2029–2040.
- (42) Rodrigues, C.; Diogo, M.; Da Silva, C.; Cabral, J. Microcarrier Expansion of Mouse Embryonic Stem Cell-Derived Neural Stem Cells in Stirred Bioreactors. *Biotechnol. Appl. Biochem.* **2011**, *58*, 231–242.
- (43) Hytönen, V.; Laitinen, O.; Airene, T.; Kidron, H.; Meltola, N.; Porkka, E.; Hörhä, J.; Paldanius, T.; Määttä, J.; Nordlund, H.; Johnson, MS.; Salminen, TA.; Airene, KJ.; Ylä-Herttuala, S.; Kulomaa, MS. Efficient Production of Active Chicken Avidin Using a Bacterial Signal Peptide in Escherichia Coli. *Biochem. J.* **2004**, *384*, 385–390.
- (44) Palma, S. I. C. J.; Fernandes, A. R.; Roque, A. C. A. An Affinity Triggered MRI Nanoprobe for pH- Dependent Cell Labeling. *RSC Adv.* **2016**, *6*, 113503–113512.
- (45) Pina, A. S.; Lowe, C. R.; Roque, A. C. A. Challenges and Opportunities in the Purification of Recombinant Tagged Proteins. *Biotechnol. Adv.* **2014**, *32*, 366–381.
- (46) Matos, M. J. B.; Pina, A. S.; Roque, A. C. A. Rational Design of Affinity Ligands for Bioseparation. *J. Chromatogr. A* **2020**, *1619*, 460871.
- (47) Branco, R. J. F.; Dias, A. M. G. C.; Roque, A.C.A. Understanding the Molecular Recognition between Antibody Fragments and Protein A Biomimetic Ligand. *J. Chromatogr. A* **2012**, *1244*, 106–115.
- (48) Santana, S.; Dhadge, V.; Roque, A. C.A. Dextran-Coated Magnetic Supports Modified with a Biomimetic Ligand for IgG Purification. *ACS Appl. Mater. Interfaces* **2012**, *4* (11), 5907–5914.
- (49) Tan, H.; Defail, A.; Rubin, J. P.; Chu, C. R.; Marra, K. G. Novel Multi-Arm PEG-Based Hydrogels for Tissue Engineering. *J. Biomed. Mater. Res. - Part A* **2010**, *92* (3), 979–987.

- (50) Lu, H. D.; Soranno, D. E.; Rodell, C. B.; Kim, I. L.; Burdick, J. A. Secondary Photocrosslinking of Injectable Shear-Thinning Dock-and-Lock Hydrogels. *Adv. Healthc. Mater.* **2013**, *2* (7), 1028–1036.
- (51) Meske, V.; Albert, F.; Ohm, T. G. Cell Cultures of Autopsy-Derived Fibroblasts. *Methods Mol. Med.* **2005**, *107*, 111-123.
- (52) Zhang, J.; Zhang, M.; Du, F.-S.; Li, Z.-C. Synthesis of Functional Polycaprolactones via Passerini Multicomponent Polymerization of 6-Oxohexanoic Acid and Isocyanides. *Macromolecules* **2016**, *49* (7), 2592–2600.
- (53) Cormio, L.; Turjanmaa, K.; Taljat, M.; Andersson, L.; M, R. Toxicity and Immediate Allergenicity of Latex Gloves. *Clin. Exp. Allergy* **1993**, *23*, 618–623.
- (54) Swistowski, A.; Peng, J.; Han, Y.; Swistowska, A. M.; Rao, M. S.; Zeng, X. Xeno-Free Defined Conditions for Culture of Human Embryonic Stem Cells, Neural Stem Cells and Dopaminergic Neurons Derived from Them. *PLoS One* **2009**, *4* (7), e6233.
- (55) Takashi, K.; Tanabe, K.; Ohnuki, M.; Narita, M.; Ichisaka, T.; Tomoda, K.; Yamanaka, S. Induction of Pluripotent Stem Cells from Adult Human Fibroblasts by Defined Factors. *Cell* **2007**, *131*, 861–872.
- (56) Kashyap, V.; Rezende, N.; Scotland, K.; Shaffer, S.; Persson, J.; Gudas, L.; Mongan, N. Regulation of Stem Cell Pluripotency and Differentiation Involves a Mutual Regulatory Circuit of the NANOG, OCT4, and SOX2 Pluripotency Transcription Factors with Polycomb Repressive Complexes and Stem Cell microRNAs. *Stem Cells Dev.* **2009**, *18*, 1093–1108.
- (57) Rizzino, A.; Wuebben, E. Sox2/Oct4: A Delicately Balanced Partnership in Pluripotent Stem Cells and Embryogenesis. *Biochem. Biophys. Acta* **2016**, *1859*, 790–791.
- (58) Shi, G.; Jin, Y. Role of Oct4 in Maintaining and Regaining Stem Cell Pluripotency. *Stem Cell Res. Ther.* **2010**, No. 1, 39.
- (59) Wang, Z.; Oron, E.; Nelson, B.; Razis, S.; Ivanonva, N. Distinct Lineage Specification

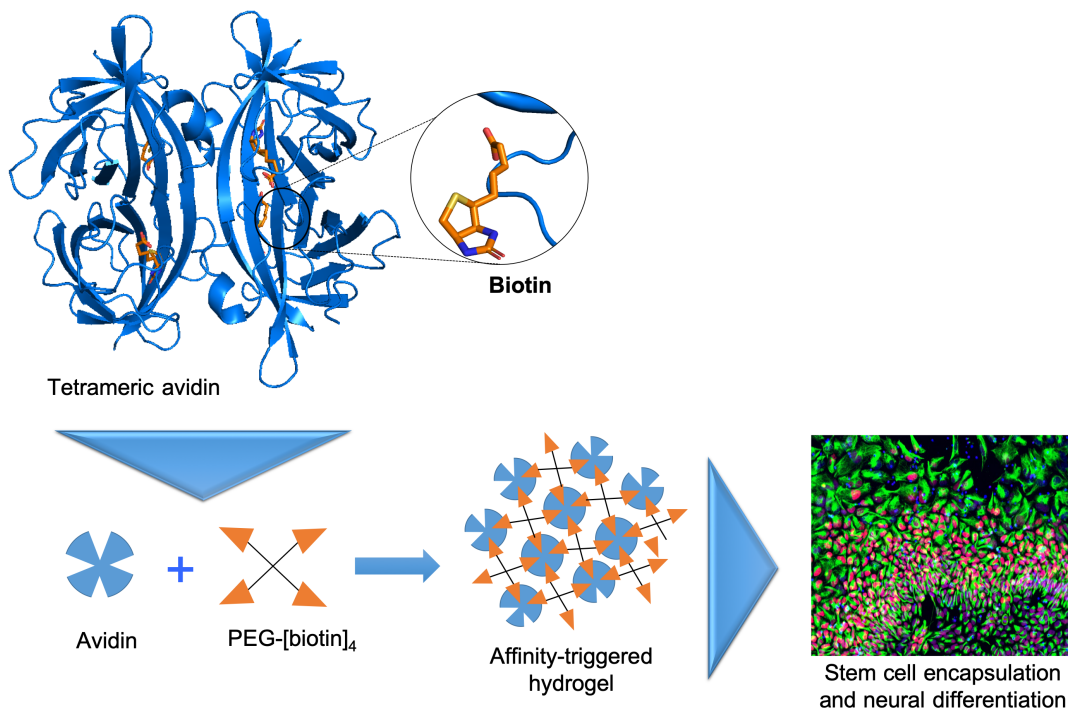
- Roles for NANOG, OCT4, and SOX2 in Human Embryonic Stem Cells. *Cell Stem Cell* **2012**, *10*, 440–454.
- (60) Adachi, K.; Suemori, H.; Yasude, S.; Nakatsuji, N.; Kawase, E. Role of SOX2 in Maintaining Pluripotency of Human Embryonic Stem Cells. *Genes Cells* **2010**, *15*, 455–470.
- (61) Zhang, X.; Huang, C.; Chen, J.; Pankratz, M.; Xi, J.; Li, J.; Yang, Y.; Lavaute, T.; Li, X.; Ayala, M.; Bondarenko, GI.; Du, ZW.; Jing, Y.; Golos, TG.; Zhang, SC. Pax6 Is a Human Neuroectoderm Cell Fate Determinant. *Cell Stem Cell* **2010**, *7*, 90–100.
- (62) Suzuki, S.; Namiki, J.; Shibata, S.; Mastuzaki, Y.; Okano, H. The Neural Stem/progenitor Cell Marker Nestin Is Expressed in Proliferative Endothelial Cells, but Not in Mature Vasculature. *J. Histochem. Cytochem.* **2010**, *58*, 721–730.
- (63) Fernandes, T.; Duarte, S.; Ghazvini, M.; Gaspar, C.; Santos, D.; Porteira, A.; Rodrigues, G.; Haupt, S.; Rombo, D.; Armstrong, J.; Sebastião, AM.; Gribnau, J.; Garcia-Cazorla, A.; Brustle, O.; Henrique, D.; Cabral, JM.; Diogo, MM. Neural Commitment of Human Pluripotent Stem Cells under Defined Conditions Recapitulates Neural Development and Generates Patient-Specific Neural Cells. *Biotechnol. J.* **2015**, *10*, 1578–1588.
- (64) Chambers, S.; Fasano, C.; Papetrou, E.; Tomishima, M.; Sadelain, M.; Studer, L. Highly Efficient Neural Conversion of Human ES and iPS Cells by Dual Inhibition of SMAD Signaling. *Nat. Protoc.* **2009**, *27*, 275–280.
- (65) Shi, Y.; Kirwan, P.; Smith, J.; Robinson, H.; Livesey, F. Human Cerebral Cortex Development from Pluripotent Stem Cells to Functional Excitatory Synapses. *Nat. Neurosciences* **2012**, *15*, 477–486.

For Table of Contents Use Only

Natural multimerization rules the performance of affinity-based physical hydrogels for stem cell encapsulation and differentiation

Cláudia Sofia Mendes Fernandes¹, André L. Rodrigues², Vitor Alves³, Tiago G. Fernandes², Ana Sofia Pina^{1}, Ana Cecília Afonso Roque^{1*}*

ToC



One of the highest affinity pairs found in Nature, avidin-biotin, is used to create affinity-triggered hydrogels, where natural multivalency must be obeyed to guide the self-assembly of robust materials. Such an approach provides the basis for the design of multicomponent hydrogels, which are important tools for mild stem cell encapsulation and differentiation, a requisite for tissue and cell therapies.